PM2.5 exposure induces renal injury via the activation of the autophagic pathway in rat and HK-2 cell

Xiaoliu Huang
Shanghai East Hospital
Jue Li (jueli1959@163.com)
Shanghai East Hospital https://orcid.org/0000-0002-5805-5229

Research

Keywords: PM2.5, Renal injury, Autophagic pathway

Posted Date: April 27th, 2020

DOI: https://doi.org/10.21203/rs.3.rs-23189/v1

Version of Record: A version of this preprint was published on July 16th, 2020. See the published version at https://doi.org/10.1186/s12302-020-00378-7.

Abstract

Background

Exposure to airborne fine particulate matter ($PM_{2.5}$) has been declared to be harmful to the human kidney. However, whether activation of the autophagic pathway plays key roles in the nephrotoxicity caused by $PM_{2.5}$ exposure is still poorly understood. The aim of this study was to explore the mechanism of kidney damage after $PM_{2.5}$ exposure in vivo and in vitro.

Results

In the present study, statistically significant alterations in water intake, urine flow rate and mean blood pressure were observed between the $PM_{2.5}$ group and FA group during the period of $PM_{2.5}$ exposure. Exposed animals showed severe edema of renal tubular epithelial cells, capillary congestion, reduction of the glomerular urinary space and early pro-fibrotic state. Moreover, significant increases in the levels of early kidney damage markers were observed in the exposed rats and these animals exhibited more apoptosis rate in kidney cells. In addition, $PM_{2.5}$ exposure resulted in the activation of the autophagic pathway, as evidenced by LC3-I to LC3-II conversion, P62 and beclin-1 activated. All of these effects are in concurrence with the presence of more autophagosomes both in vivo and in vitro after $PM_{2.5}$ exposure.

Conclusions

Taken together, our findings indicated that $PM_{2.5}$-induced renal injury via the activation of the autophagic pathway in renal tubular epithelial cells.

Background

A report on the world health organization (WHO) in 2016 estimated that nearly 3 million people die every year due to air pollution related diseases (Tavera Busso et al., 2018). $PM_{2.5}$ refers to the complex mixture small particles and liquid droplets with aerodynamic diameter ≤ 2.5 μm in the atmosphere, and is an important indicator for assessing air pollution (Tavera Busso et al., 2018; Zhou et al., 2019). $PM_{2.5}$ mainly deposits in lung tissues after inhaling the respiratory tract, and can even diffuse in the blood circulation system through the alveolar-capillary barrier, affecting distal organs such as liver and kidneys (Li et al., 2019a; Pinkerton et al., 2000). Zhang et al, found that severe histopathological changes in hepatocyte edema and glomerular atrophy occurred in rats induced by intratracheal instillation of $PM_{2.5}$ (Zhang et al., 2017). Recently, some recent epidemiological studies have reported a strong and consistent association between $PM_{2.5}$ exposure and renal function decline (Chen et al., 2018; Mehta et al., 2016). Bowe et al, estimated that the global burden of incident chronic kidney disease (CKD) attributable to $PM_{2.5}$ was about 6.95 million in 2016, and air pollution may be an important risk factor for the prevalence of kidney

disease (Bowe et al., 2019). Experimental studies have also shown that mid-/long-term exposure to high levels of $PM_{2.5}$ can induce kidney damage in rodent models (Aztatzi-Aguilar et al., 2016; Ge et al., 2018).

Although the respiratory system is the primary target organ for toxicity of $PM_{2.5}$ exposure, epidemiological evidence has indicated that $PM_{2.5}$ exposure is an important risk factor for cardiovascular morbidity and mortality (Brook et al., 2010). The strong correlation between chronic kidney disease and cardiovascular disease has been demonstrated by both observational studies and a meta-analysis (Moody et al., 2012). In conditions of renal insufficiency and in patients undergoing dialysis is prone to cardiovascular diseases have been reported in clinical practice, which indicates a potential interaction between the kidney and the cardiovascular system (Aztatzi-Aguilar et al., 2016). Tavera Busso et al, in a spontaneously hypertensive rat (SHR) model after subchronic exposure to $PM_{2.5}$, observed more severe alterations of fibrosis, mesangial expansion, tubular epithelial cells detachment, decrease glomerular and tubular lumen volumes than healthy animals (Tavera Busso et al., 2018). Moreover, Yan et al, histological analysis showed $PM_{2.5}$ advanced glomerulosclerosis and a punctual tubular damage of the kidney in a diabetic rat model after subchronic exposure to $PM_{2.5}$ (Yan et al., 2014). Endothelial dysfunction is viewed as one of the common pathophysiological mechanisms in cardiovascular disease and chronic kidney disease (Stam et al., 2006). Aztatzi-Aguilar et al, early kidney damage induced by subchronic exposure to $PM_{2.5}$ in rats showed angiotensin/bradykinin systems imbalance and a statistically significant increment in median blood pressure (Aztatzi-Aguilar et al., 2016). At present, studies have confirmed that autophagy of cardiovascular endothelial was the potential mechanism of $PM_{2.5}$-induced cardiovascular dysfunction (Ding et al., 2017; Wang et al., 2017a; Zhou et al., 2018). In contrast, the contribution of $PM_{2.5}$ exposure to endothelial damage in kidneys via autophagic pathway has not been adequately studies at a cellular and molecular levels.

Autophagy is a physiological process whereby eukaryotic cells undergo self-digestion, which allows the degradation and recycling of unnecessary intracellular proteins and dysfunctional organelles via the autophagosome and lysosomes (Deng et al., 2013; Deng et al., 2014a; Su et al., 2017). The formation of the autophagosome involves the action of multiple autophagy-related genes (Atgs), such as Beclin-1(Atg6), and microtubule-associated proteins light chain 3 (LC3) (Deng et al., 2013; Zhang et al., 2018b). Sequestosome1/P62 (SQSTM1) is a regulatory autophagy protein originally identified as a binding protein for nonreceptor-type tyrosine kinase $P56^{Lck}$ (Ishii et al., 2013). Moreover, P62 has been found to be key roles in the selective autophagy signaling pathway because of interacting with both Keap1 and LC3 (Ichimura et al., 2013; Zhou et al., 2018). Autophagy is considered to be an adaptive response to stress, and plays an important role in maintaining cellular homeostasis during pathogenic conditions and diseases, as well as regulating caspase-independent cell death (Deng et al., 2014a; Zhou et al., 2018).

The kidney is an organ with a rich and diverse endothelial cell (EC) populations (Verma and Molitoris, 2015). Ding et. al, found that gold nanoparticles could induce autophagy of hypoxia HK-2 cells (Ding et al., 2014). Take into account this, we hypothesized that $PM_{2.5}$ exposure induced autophagy of renal endothelial cells leading to deterioration of renal function. In this study, our aim was to use SD rats

studying the effects of $PM_{2.5}$ on kidney damage by a natural inhalation exposure systems, and human proximal tubule epithelial cell (HK-2) was chosen as a vitro model to further investigate the potential mechanism triggered by $PM_{2.5}$ exposure to renal dysfunction. Moreover, kidney injury molecule type-1(KIM-1), which a specific biomarker of damage to tubular cells was detected to assess renal injury after $PM_{2.5}$ exposure. Here, our findings would provide important insight into the involvement of $PM_{2.5}$ pollution in kidney damage.

Material And Methods

Animal maintenance

4-week-old Sprague-Dawley male rats were purchased from Jiexijie experimental animal co., LTD. (Shanghai, China). All animals were kept in a standard clean room at a temperature of 22-24℃ with 50-60% relative humidity and a 12-hour day/night cycle. Rats were allowed to drink and eat freely, except when kept in the a metabolic cage. After one-week acclimation, rats were randomly divided into (FA, exposure to filtered air) group or ($PM_{2.5}$, exposure to concentrated $PM_{2.5}$) group. The study was subject to approval by the institutional animal care and use committees of Tongji University.

$PM_{2.5}$ exposure system

A natural inhaled $PM_{2.5}$ exposure system (Shanghai-MRTAS, patent #201510453600.8-) provided by the meteorological service of Shanghai. Concentrated particulate matter of the exposure system was generated using a versatile aerosol concentration enrichment system (VACES) as previously described (Li et al., 2019b; Wang et al., 2018). The $PM_{2.5}$ exposure system which basically keeps the chemical properties of $PM_{2.5}$ before concentration is located at the school of public health, Fudan university (130 Dong 'an Road, Shanghai, China), where ambient $PM_{2.5}$ particles come mainly from traffic exhaust. The exposure experiments were performed for eight hours per day, five consecutive days per week from October 2018 to January 2019. Two $PM_{2.5}$ monitors (PDR-1500,Thermo Scientific) that were connected to the air inlets of the exposure and control chambers via filtered air were used to measure the Real-time concentrations of $PM_{2.5}$, and simultaneously followed by sampling the $PM_{2.5}$ on filters to determined the accurate concentrations.

Metabolic cage

After 5-day exposure, rats were placed in metabolic cages (Yuyan instrument, China) for 24h each week. During the twenty-hour period, food was not given to avoid contamination of the urine. The urine was harvested, estimated the water intake and calculated the urinary flow. These data were adjusted for body weight.

Measurement of blood pressure

Medlab biological signal acquisition and processing system (Nanjing Calvin biotechnology, China) was used to record blood pressure. The animals were first fixed in the sleeve and warmed to a suitable temperature prior to each measurement to ensure adequate diastolic blood pressure. Then, more than three blood pressure measurements using a cutoff ring and a transducer placed on the proximal heart of the tail were performed when the animal was keeping quiet. Basal measurement was evaluated one day before the initiation of the 12-week exposure and on the seventh day after every weekly exposure, with a metabolic cage period of one day for the animals to rest and hydrate. According to the previous study calculated the mean blood pressure (MBP) as follows (Aztatzi-Aguilar et al., 2016):

MBP =diastolic pressure+0.33 (systolic pressure-diastolic pressure)

Histology

Renal tissues fixed with formaldehyde for more than 24 hours were dehydrated with alcohol, clarified by xylene and embedded in paraffin. Slides were cut and stained with Hematoxylin&eosin (HE) stain and Masson's Trichrome stain. Then, the images were observed and captured by an optical microscope (Olympus, Japan).

Transmission electron microscopy

Treated cells and kidney tissues were immediately fixed in 2.5% glutaraldehyde at 4℃, then washed 3 times with 0.1M PBS and underwent 2 h post-fixation in osmic acid at room temperature. Subsequently, cells were washed 3 times with 0.1M PBS, then dehydrated in a graded alcohol series and embedded in epoxy resin. Then ultrathin serial sections (60-100nm) of embedded samples were cut using ultra-microtomy (Leica, EM UC7, Germany), then stained with uranyl acetate and lead citrate, and examined under an electron microscope (Tecnai G^2 20 TWIN, FEI Company, USA) at 200 kv.

Apoptosis assay

The TdT-mediated dUTP nick labeling (TUNEL) technique was used for the determination of cell apoptosis in kidney tissues. Slides of kidney were deparaffinized, and a TUNEL assay kit (Roche, Shanghai, China) was used to detect the apoptosis according to the manufacture's instructions. Images were observed and captured using a fluorescent microscope (Nikon, Japan).

Cells and culture

Human proximal tubule epithelial cells (provided by Professor Andong Qiu, School of Life Sciences and Technology, Tongji University, Shanghai, China) were cultured in DMEM/F12 (Biological Industries, Israel) supplemented with 10% (*v/v*) fetal bovine serum (Gibco, Grand Island, NY) and 1% (*v/v*) penicillin/streptomycin (Solarbio, China). Exponentially growing cells were maintained at 37°C in a humidified incubator containing 5% CO_2, with daily replacement of the cell culture medium. Cells were washed with phosphate-buffered saline (PBS), digested with 0.25% trypsin (Solarbio, China) and seeded in new culture flasks/dishes after they reached 80% confluence.

Real time-quantitative PCR analysis

Total RAN of the kidney cortex was isolated using Trizol reagent (Invitrogen) according to the manufacturer's instructions. The cDNA was used as a template to examine the mRNA expression levels of target genes using SYBR® Green mixture (Takara, Dalian, China) on an ABI QuantStudio 7 detection system (Applied Biosystems, USA). GAPDH was taken as an internal control and the gene expressions were assessed using the $2^{-\Delta\Delta Ct}$ method. The PCR cycle was as follows: initial denaturant at 95 ℃ for 6 min, followed by 40 cycles of denaturing at 95 ℃ for 10 s, and annealing at 60 ℃ for 34 s. The primer sequences for real-time PCR were shown as following: (5'→3'): Rat-GAPDH forward GCCTTCCGTGTTCCTACC reverse CCTGCTTCACCACCTTCTT; Rat-KIM-1 forward GAGGTGGAGACTCTGGTTGA reverse TGGAGATTCCTGGATGGT; Rat-TGF-β forward CTAATGGTGGACCGCAACAAC reverse CACTGCTTCCCGAATGTCTGA; Rat-Smad2 forward ACCACTCTCTCCCCTGTCAATCA reverse AACCTAAGCAGAACCTCTCCGA.

Western blot analysis

Total protein of kidney tissues and cells was lysed in ice-cold NP40 buffer (Beyotime, China) containing protease and phosphatase inhibitors. Then, the liquid supernatants were collected by centrifugation at 12000*g* for 15 min at 4°C, and the protein concentrations were calculated using a BCA protein quantification kit (Beyotime, China). The protein samples were subjected to 15% sodium dodecyl sulfate polypropylene gel electrophoresis (SDS-PAGE) and transferred onto polyvinylidene difluoride (PVDF) membranes (Millipore, MA, USA). The PVDF membranes were then blocked in 5% non-fat milk at room temperature for 1 h, incubated with specific primary antibodies KIM-1 (Cell Signaling Technology, USA), LC3, Beclin-1, P62, GAPDH and β-actin (Proteintech, USA) at 4°C overnight, and subsequently incubated with HRP-conjugated secondary antibodies (Proteintech, USA) at room temperature for 1 h. After washing with TBST, the protein bands were visualized using an enhanced chemiluminescence system (Image Quant LAS, 4000 mini). Protein expression was quantified using ImageJ software (version 1.4.2b, USA) and standardized to the expression of a housekeeping gene and is given in the fold change compared to that in the control samples.

Data analysis

Data was expressed as mean ± standard deviation (SD). Statistical analyses were performed using SPSS Statistical 19.0 software (IBM, USA).Independent-sample *t* test was used to compare the difference between $PM_{2.5}$ and FA groups. Statistical analysis between multi-groups were analyzed by one-way analysis of variance (ANOVA) followed Duncan's multiple-comparison tests. *P*-Value < 0.05 was considered statistically significant.

Results

Exposure description and hydration state

During exposure periods, the mean concentration of $PM_{2.5}$ outdoor (Xujiahui District, Shanghai) was 41.48 ug /m^3 (19.2–83.8 ug /m^3), the average concentration in the exposed chamber was 255.71 ug /m^3 (72.15-596.84 ug /m^3) and 8.24 ug /m^3 (4.52–13.54 ug /m^3) in the control chamber, respectively. The average concentration of particulate enrichment was 6.16 times (2.91–13.69 times). These results showed that the concentration effects of $PM_{2.5}$ in exposed chamber were affected by $PM_{2.5}$ concentration in outdoor air, which was consistent with the dynamic change of outdoor concentration (Fig. 1.A). During the 12 weeks of exposure, the animals' body weight was recorded every weekend. The results showed that there was no statistical difference between the FA and $PM_{2.5}$ groups (Fig. 1.B). In addition, water intake and urinary flow rates were measured during the 24-hour period. According to the results (Fig. 1.C), during the exposure period, the water consumption of animals in the $PM_{2.5}$ group was higher than that of the FA group, and there was a significant difference in the eighth, tenth and eleventh weeks ($p < 0.05$). Meanwhile, the results showed (Fig. 1.D) that the urinary flow rate of the $PM_{2.5}$ group was higher than that of the FA group, along with significant difference in all weeks except the first, second and twelfth weeks ($p < 0.05$).

Changes of Mean blood pressure

In this study, mean blood pressure (MBP) was used as a physiological parameter of vascular tone, which can be an indicator of perfusion pressure of organs. Therefore, founded on the assessment of the basic blood pressure of the animals in each group, we measured the tail blood pressure of the animals after weekly exposure. As can be seen from Table1, in the 5th, 7th, 8th, 10th and 12th week after exposure, the mean blood pressure of the $PM_{2.5}$ group was significantly higher than that of the FA group ($p < 0.05$), and there was no difference in other weeks. These results indicated that $PM_{2.5}$ exposure could affect vascular tone of experimental animals and probably the perfusion of organs.

Table 1
Mean blood pressure measurements after exposure to $PM_{2.5}$

Weeks	The mean blood pressure (MBP)		
	$PM_{2.5}$	FA	*p*-value
Basal	78.97 ± 0.96	77.51 ± 0.55	0.202
WK-1	77.72 ± 1.04	79.98 ± 0.94	0.131
WK-2	84.16 ± 0.89	84.10 ± 1.14	0.969
WK-3	84.92 ± 0.83	86.24 ± 0.83	0.281
WK-4	101.99 ± 3.37	102.86 ± 2.12	0.601
WK-5	109.53 ± 1.20	101.09 ± 1.76	0.002
WK-6	105.24 ± 1.79	104.97 ± 1.31	0.904
WK-7	112.41 ± 1.62	106.16 ± 1.05	0.006
WK-8	112.61 ± 1.38	105.91 ± 1.23	0.003
WK-9	105.34 ± 2.38	106.83 ± 3.36	0.727
WK-10	110.81 ± 1.33	104.93 ± 1.25	0.005
WK-11	108.50 ± 1.51	107.42 ± 1.41	0.641
WK-12	114.46 ± 1.34	108.09 ± 0.91	0.001

Histology and pro-fibrotic state

After exposure to $PM_{2.5}$ for 12 weeks, pathological changes of H&E-stained renal tissue samples showed the severe edema of renal tubular epithelial cells, capillary congestion and reduction of the glomerular urinary space, whereas the normal structures of glomerulus and tubular can be observed in the FA group (Fig2.A). In addition, to further evaluate renal injury, we used Western blotting and RT-PCR to examine the protein and gene mRNA expression of KIM-1, a marker of early renal injury. Shown as figure (Fig2.C-D), mRNA expression of KIM-1 in renal cortex of $PM_{2.5}$ group was significantly higher than those of FA group ($p<0.01$), and levels of KIM-1 protein in serum of $PM_{2.5}$ group was significantly higher than those of FA group ($p<0.01$).

Masson's Trichromic staining was further used to estimate the changes of collagen deposition in renal tissue induced by $PM_{2.5}$ exposure. As showing in (Fig3.A), compared with the control group, significant collagen deposition was observed in the kidney tissues of the $PM_{2.5}$ group. mRNA expression levels of TGF-β and Smad2 were analyzed as inducers of early pro-fibrosis (Fig3.B). We observed that mRNA

expression levels of TGF-β and Smad2 in renal cortex of $PM_{2.5}$ group were significantly higher than those of FA group ($p<0.05$).

$PM_{2.5}$ induced renal cell apoptosis of rats

The TUNEL method was used to further determine whether $PM_{2.5}$ exposure could induce cell apoptosis in renal tissues. These results showed that green fluorescence points in renal tissues in the $PM_{2.5}$ group were significantly more than those in the FA group (Fig3. A). Compared with FA group, the proportion of apoptosis cells in $PM_{2.5}$ group showed significantly statistical difference ($p<0.01$) (Fig3. B).

$PM_{2.5}$ induced increase of autophagy and changes of autophagic protein expression in renal tissues.

As can be observed in the figure5, there were multiple layers (myeloid) of exposed animal renal tissue cells. To further clarify whether $PM_{2.5}$ activated autophagy signaling related molecules in renal cells, Western blotting was used to analyze the expression levels of LC3, P62 and beclin-1 proteins. Our results showed that compared with FA group, protein signals of LC3 and P62 in $PM_{2.5}$ group was significantly down-regulated, while protein signals of beclin-1 were significantly up-regulated (Fig 6). Statistical analysis results showed that the ratio of LC3II/LC3I and beclin-1 protein abundance in $PM_{2.5}$ group were significantly higher than those in the FA group, and the protein abundance of P62 was significantly lower than that in the FA group. Collectively, $PM_{2.5}$ exposure triggered the intracellular autophagy signaling pathway in renal tissue.

Morphological changes following $PM_{2.5}$ treatment in HK-2 cells

We further examined the morphology of HK-2 cells following treatment with $PM_{2.5}$ using transmission electron microscopy (TEM). Untreated control HK-2 cells presented typical cellular morphology, including normal sized nucleus, even distribution of microvilli on the cell surface. In contrast, HK-2 cells that were treated with $PM_{2.5}$ (400 μg/mL) displayed an absence of microvilli on the surface of the cell membrane, along with an obvious swelling of the nucleus, and destruction of the cell membrane lysis. Moreover, high magnification images showed the presence of numerous autophagic vacuoles, early autophagic vacuoles, degradation autophagic vacuoles.

$PM_{2.5}$ induced the activation of autophagic pathways in HK-2 cells

In order to determine whether $PM_{2.5}$ treatment also induced the activation of autophagic pathways in HK-2 cells, we examined the expression of LC3, which contains two species including activated LC3-I and processed IL3-II, as well as P62 and Beclin1 using Western blot analyses. $PM_{2.5}$ treatment resulted in a significant increase in the ratio of LC3-II to LC3-I content in a dose- and time-dependent manner, indicating that $PM_{2.5}$ exposure induced the conversion of LC3-I to processed LC3-II (Fig8). Moreover, $PM_{2.5}$ treatment significantly up-regulated protein expression levels of P62 and Beclin1 compared to untreated control

cells. Collectively, these findings demonstrated that $PM_{2.5}$ induced the activation of the cascade of LC3, P62 and Beclin1 proteins involved in the autophagic pathway in HK-2 cells.

Discussion

In the present study, the artificial climatic environment exposure system (Shanghai-METAS) was used to study the effects of $PM_{2.5}$ exposure on kidney damage. This equipment which could maximally simulate "real world" $PM_{2.5}$ exposure is the first comprehensive animal exposure system established in China, and has been effectively used to assess the effects of $PM_{2.5}$ exposure on health and diseases development in rodent in several studies (Du et al., 2018; Wang et al., 2018; Xu et al., 2019). Interestingly, the results of this study also confirmed that subchronic exposure to $PM_{2.5}$ led to kidney damage in SD rats.

As the principal organ of the body, the kidney has important physiological functions such as urinary production, excretion/reabsorption, acid-alkaline homeostasis and endocrine function. To investigate whether hydration state of the kidney is affected by $PM_{2.5}$ exposure, the water consumption and urine volume of the animals within 24 hours once a week was recorded during the exposure period. As showing in Fig. 1.C-D, the alterations of water intake and urinary flow rate were observed between $PM_{2.5}$ and FA groups after exposure to $PM_{2.5}$, and the results were consistent with the previous report (Aztatzi-Aguilar et al., 2016). The stimulating effects of $PM_{2.5}$ hygroscopic properties and nervous system, as well as adequate water needed in lung tissues to clean up the harm of $PM_{2.5}$ particle deposition for self-protection might be the main reasons for the increases of water consumption in rodent after $PM_{2.5}$ exposure (Aztatzi-Aguilar et al., 2016). Moreover, it has been shown that administration of Cisplatin (CP) or CP + Cerium oxide nanoparticles (CeO2 NPs) in rats increased the water intake and urine volume compared with saline, indicated that the damaged renal tubular could cause the deterioration of capacity of tubular cells to reabsorb water, and subsequent polyuria leading to dehydration (Nemmar et al., 2019). Similarly, the increase of urine volume was one of the nephrotoxicity characteristics in an acute renal failure (ARF) rat model induced by gentamicin in a study about a plant extracts for the prevention and attenuation of ARF (Ehsani et al., 2017). These results suggested that the physiological functions of the kidney were damaged, resulting in an imbalance of hydration state after exposure to $PM_{2.5}$. However, the body weight of rats in both groups has been not affected during the exposure to $PM_{2.5}$ period in this study (Fig. 1.B).

$PM_{2.5}$ exposure increased the risk of cardiovascular disease (Huang et al., 2018). Vascular endothelial cells are the primary vascular barrier to local damage factors induced by exposure to $PM_{2.5}$, such as inflammatory factors and free radicals, as well as toxic and harmful substances of $PM_{2.5}$ (Feng et al., 2016). Vascular endothelium play key roles in regulating blood pressure, atherosclerosis and thrombosis, and $PM_{2.5}$ exposure can lead to structural and functional impairment of vascular endothelial cells (Pope et al., 2016). For this reason, we monitored MBP during animal exposure as an indicator of vascular response to $PM_{2.5}$ to assess the effects of $PM_{2.5}$ on peripheral blood pressure and organ blood perfusion.

Our results showed that there was no difference in the basal blood pressure between the two groups. But in the 5th, 7th, 8th, 10th and 12th weeks, the MBP of the $PM_{2.5}$ group was significantly higher than that of the FA group ($p < 0.05$) after subchronic exposure to $PM_{2.5}$. Because of the close relationship between the physiological function of the kidney and systemic blood pressure, an increase in MBP could cause the renal peritubular capillaries damage.

Currently, a few studies have described that exposure to $PM_{2.5}$ could cause the pathological alterations of kidney tissues (Aztatzi-Aguilar et al., 2016; Ge et al., 2018; Tavera Busso et al., 2018). Here, both in vivo and in vitro experiments showed that the morphological structures of renal tissues and HK-2 cells were damaged after $PM_{2.5}$ exposure. H&E staining results of tissue sections showed that damage in tubular and glomerular was observed as evidenced by the severe edema of renal tubular epithelial cells, capillary congestion and reduction of the glomerular urinary space (Fig. 2.A). Moreover, $PM_{2.5}$ treatment resulted in significant changes in cellular morphology in HK-2 cells, including destruction of the cell membrane lysis and swelling of the nucleus (Fig. 7). Similar histopathologic changes have been reported in diabetic nephropathy and acute kidney injury (Chen et al., 2014; Yan et al., 2014). KIM-1 is a transmembrane glycoprotein whose extracellular segments can be shed, and the levels in urine are often detected in clinical or experimental studies to diagnose acute kidney injury or early kidney damage (Khreba et al., 2019; Tanase et al., 2019; Zhang et al., 2017). In this study, the significant increase of KIM-1 protein expression in serum and KIM-1 mRNA expression in kidney tissues were observed after $PM_{2.5}$ exposure in vivo experiment(Fig. 2.B-D). Thus, these results indicated that exposure to $PM_{2.5}$ induced damage to the proximal tubule epithelium.

Our results showed that during the 12-week period of exposure to $PM_{2.5}$, kidney tissue experienced sustained damage, but the body also activated a response to repair the damage. After the end of exposure, mRNA expression of TGF-β in renal tissues of the $PM_{2.5}$ group was increased. TGF-β plays an important role in participating in post-injury repair of tissues by promoting the deposition of extracellular matrix components such as collagen (Ismaeel et al., 2019). But prolonged, uncontrolled TGF-β activation can lead to an overdose of extracellular matrix, leading to tissue fibrosis (Rauchman and Griggs, 2019). An increase of collagen deposition in renal tissue was observed by Masson's Trichromic staining in this study. We speculated that long-term exposure to $PM_{2.5}$ could lead to renal damage, but the body could induce collagen deposition through activation of TGF-β components to promote damage repair. However, the increased mRNA expression of Smad2 gene in renal tissues suggested that long-term exposure to $PM_{2.5}$ may promote pro-fibrosis and renal dysfunction. Similarly, TGF-β1 and Smad2 played an important role in the process of renal fibrosis have been confirmed in previous studies. (Meng et al., 2015; Meng et al., 2010).

In order to investigate the renal damage of SD rats exposed to $PM_{2.5}$ at the cellular level, we first used transmission electron microscopy to observe the changes in renal cell microstructure. The results showed that there were lysosome vacuoles and multilayer (myeloid) substances in the cytoplasm of the kidney tissues of the exposed group. Moreover, TUNEL analysis was used to further analyze the degree of cell

damage in kidney tissues, our results showed that apoptosis responses were observed significantly in $PM_{2.5}$ exposured rats. Previous studies suggested that apoptosis in renal tubular cells was considered as a causal factor in the development of kidney diseases/injury (Song et al., 2018; Zhang et al., 2019). Many in vivo and in vitro experiments have confirmed that $PM_{2.5}$ induced inappropriate apoptosis (too much) is one of the potential mechanisms of $PM_{2.5}$ health hazards (Liu et al., 2019; Wang et al., 2017b; Zhang et al., 2018a; Zhou et al., 2014). Therefore, we speculated that $PM_{2.5}$ may enter the kidney through blood circulation, and then accumulate in cells, resulting in kidney damage.

As previously known, obvious autophagosomes and lysosome vacuoles were found in the cytoplasm of HK-2 cells after exposure by transmission electron microscopy. Autophagy refers to the catabolic process of self-digestion of abnormal substances in the cytoplasm of cells by lysosomes (Condello et al., 2019). Beclin-1 plays a key role in early autophagosome formation, followed by LC3 which is a significant feature of autophagy level. P62 is an intracellular multifunctional protein acting on selective autophagy, which is mainly induced by stress and involved in a variety of signal transduction, including in the formation process of autophagosomes, as a bridge between LC3 and polyubiquitin protein, it can regulate the transport of damaged mitochondria into autophagosomes and degradation, and has an important regulatory role in the Nrf2/Keap1 signaling pathway. Studies have found that autophagy induced by $PM_{2.5}$ in human umbilical vein endothelial cells (HUVECs) and human lung epithelial cells (A549) is characterized by significant increase in LC3-II and beclin-1 expression levels and LC3-II/LC3-I ratio (Deng et al., 2014b; Ding et al., 2017). Our results showed that after exposure to $PM_{2.5}$, LC3-I to LC3-II conversion, P62, and beclin-1 were activated. The increased expression of P62 indicates that intracellular autophagy flow is blocked, which may be related to the involvement of P62 in activating the Nrf2/Keap1 signaling pathway, because the dissociation of Nrf2/Keap1 requires P62 binding, which further confirms that $PM_{2.5}$ induces the production of excessive ROS in HK-2 cells. In animal exposure experiments, the LC3-II/LC3-I ratio and beclin-1 protein expression level of the $PM_{2.5}$ group were significantly higher than those of the FA group, while the P62 protein expression level of the $PM_{2.5}$ group was significantly lower than that of the FA group. These results showed that $PM_{2.5}$ exposure led to the occurrence of autophagy and autophagy flow in renal tissues. The results suggested that P62 was a selective regulatory protein, and autophagy played an important role in $PM_{2.5}$ induced HK-2 cytotoxicity and renal injury.

Conclusion

In summary, the present study demonstrated that $PM_{2.5}$ exposure could promote autophagy of kidneys, especially renal tubular epithelial cells both in vitro and vivo. We further provided evidence that autophagy pathway was crucial for the progression of kidney damage induced by $PM_{2.5}$ exposure, which was most likely via the activation of LC3, Beclin-1 and P62 expressions. Our findings provided insight about the effects and mechanism of $PM_{2.5}$ on renal injury.

Abbreviations

Fine particulate matter ($PM_{2.5}$);

Human proximal tubule epithelial cells (HK-2);

Kidney injury molecule-1 (KIM-1);

TdT-mediated dUTP nick labeling (TUNEL);

Mean blood pressure (MBP);

Autophagy-related genes (Atgs);

Microtubule-associated proteins light chain 3 (LC3);

Sequestosome1(P62);

Quantitative Real-time PCR (qPCR)

Declarations

Acknowledgements

None applicable.

Funding

This study was funded by the Shanghai Key Laboratory of Meteorology and Health (Grant Nos.: QXJK201612 and QXJK201805), and Science and Technology program of education department of Jiangxi province (GJJ180573).

Availability of data and materials

The datasets obtained and analyzed in the current study are available from the corresponding author on reasonable request.

Authors' contributions

XH was involved the experiments, data processing and analysis, and manuscript writing. JL designed the study and contributed to modification of the manuscript. All authors read and approved the final manuscript.

Ethics approval and consent to participate

The study was subject to approval by the institutional animal care and use committees of Tongji University.

Consent for publication

Not applicable.

Competing interests

The authors declare that all authors have no conflicts of interest related to this manuscript.

Author details

[1]Shanghai East Hospital, Tongji University School of Medicine, Shanghai 200092, China

[2] Jinggangshan University School of Medicine, Jiangxi 343009, China.

[3] Institute of Clinical Epidemiology and Evidence-based medicine, Tongji University School of Medicine, Shanghai 200092, China.

[4] Key Laboratory of Arrhythmia, Ministry of Education, East Hospital, Tongji University School of Medicine, Shanghai 200092, China.

References

Aztatzi-Aguilar, O.G., Uribe-Ramirez, M., Narvaez-Morales, J., De Vizcaya-Ruiz, A., Barbier, O., 2016. Early kidney damage induced by subchronic exposure to PM2.5 in rats. Part Fibre Toxicol 13, 68.

Bowe, B., Xie, Y., Li, T., Yan, Y., Xian, H., Al-Aly, Z., 2019. Estimates of the 2016 global burden of kidney disease attributable to ambient fine particulate matter air pollution. BMJ Open 9, e022450.

Brook, R.D., Rajagopalan, S., Pope, C.A., Brook, J.R., Bhatnagar, A., Diez-Roux, A.V., Holguin, F., Hong, Y., Luepker, R.V., Mittleman, M.A., Peters, A., Siscovick, D., Smith, S.C., Whitsel, L., Kaufman, J.D., 2010. Particulate Matter Air Pollution and Cardiovascular Disease. Circulation 121, 2331-2378.

Chen, L., Marko, L., Kassmann, M., Zhu, Y., Wu, K., Gollasch, M., 2014. Role of TRPV1 channels in ischemia/reperfusion-induced acute kidney injury. PLoS One 9, e109842.

Chen, S.Y., Chu, D.C., Lee, J.H., Yang, Y.R., Chan, C.C., 2018. Traffic-related air pollution associated with chronic kidney disease among elderly residents in Taipei City. Environ Pollut 234, 838-845.

Condello, M., Pellegrini, E., Caraglia, M., Meschini, 2019. Targeting Autophagy to Overcome Human Diseases. Int J Mol Sci 20, 725.

Deng, X., Zhang, F., Rui, W., Long, F., Wang, L., Feng, Z., Chen, D., Ding, W., 2013. PM2.5-induced oxidative stress triggers autophagy in human lung epithelial A549 cells. Toxicol In Vitro 27, 1762-1770.

Deng, X., Zhang, F., Wang, L., Rui, W., Long, F., Zhao, Y., Chen, D., Ding, W., 2014a. Airborne fine particulate matter induces multiple cell death pathways in human lung epithelial cells. Apoptosis 19, 1099-1112.

Deng, X., Zhang, F., Wang, L., Rui, W., Long, F., Zhao, Y., Chen, D., Ding, W., 2014b. Airborne fine particulate matter induces multiple cell death pathways in human lung epithelial cells. Apoptosis 19, 1099-1112.

Ding, F., Li, Y., Liu, J., Liu, L., Yu, W., Wang, Z., Ni, H., Liu, B., Chen, P., 2014. Overendocytosis of gold nanoparticles increases autophagy and apoptosis in hypoxic human renal proximal tubular cells. International Journal of Nanomedicine, 4317.

Ding, R., Zhang, C., Zhu, X., Cheng, H., Zhu, F., Xu, Y., Liu, Y., Wen, L., Cao, J., 2017. ROS-AKT-mTOR axis mediates autophagy of human umbilical vein endothelial cells induced by cooking oil fumes-derived fine particulate matters in vitro. Free Radic Biol Med 113, 452-460.

Du, X., Jiang, S., Zeng, X., Zhang, J., Pan, K., Zhou, J., Xie, Y., Kan, H., Song, W., Sun, Q., Zhao, J., 2018. Air pollution is associated with the development of atherosclerosis via the cooperation of CD36 and NLRP3 inflammasome in ApoE(-/-) mice. Toxicol Lett 290, 123-132.

Ehsani, V., Amirteimoury, M., Taghipour, Z., Shamsizadeh, A., Bazmandegan, G., Rahnama, A., Khajehasani, F., Fatemi, I., 2017. Protective effect of hydroalcoholic extract of Pistacia vera against gentamicin-induced nephrotoxicity in rats. Ren Fail 39, 519-525.

Feng, S., Gao, D., Liao, F., Zhou, F., Wang, X., 2016. The health effects of ambient PM2.5 and potential mechanisms. Ecotoxicol Environ Saf 128, 67-74.

Ge, C., Xu, M., Qin, Y., Gu, T., Lv, J., Wang, M., Wang, S., Ma, Y., Lou, D., Li, Q., Hu, L., Tan, J., 2018. iRhom2 loss alleviates renal injury in long-term PM2.5-exposed mice by suppression of inflammation and oxidative stress. Redox Biol 19, 147-157.

Huang, W., Wang, L., Li, J., Liu, M., Xu, H., Liu, S., Chen, J., Zhang, Y., Morishita, M., Bard, R.L., Harkema, J.R., Rajagopalan, S., Brook, R.D., 2018. Short-Term Blood Pressure Responses to Ambient Fine Particulate Matter Exposures at the Extremes of Global Air Pollution Concentrations. Am J Hypertens 31, 590-599.

Ichimura, Y., Waguri, S., Sou, Y.-s., Kageyama, S., Hasegawa, J., Ishimura, R., Saito, T., Yang, Y., Kouno, T., Fukutomi, T., Hoshii, T., Hirao, A., Takagi, K., Mizushima, T., Motohashi, H., Lee, M.-S., Yoshimori, T., Tanaka, K., Yamamoto, M., Komatsu, M., 2013. Phosphorylation of p62 Activates the Keap1-Nrf2 Pathway during Selective Autophagy. Molecular Cell 51, 618-631.

Ishii, T., Warabi, E., Siow, R.C.M., Mann, G.E., 2013. Sequestosome1/p62: A regulator of redox-sensitive voltage-activated potassium channels, arterial remodeling, inflammation, and neurite outgrowth. Free Radical Biology and Medicine 65, 102-116.

Ismaeel, A., Kim, J.-S., Kirk, J.S., Smith, R.S., Bohannon, W.T., Koutakis, P., 2019. Role of Transforming Growth Factor-β in Skeletal Muscle Fibrosis: A Review. Int J Mol Sci 20, 2446.

Khreba, N.A., Abdelsalam, M., Wahab, A.M., Sanad, M., Elhelaly, R., Adel, M., El-Kannishy, G., 2019. Kidney Injury Molecule 1 (KIM-1) as an Early Predictor for Acute Kidney Injury in Post-Cardiopulmonary Bypass (CPB) in Open Heart Surgery Patients. Int J Nephrol 2019, 6265307.

Li, D., Li, Y., Li, G., Zhang, Y., Jiang Li, J., Chen, H., 2019a. Fluorescent reconstitution on deposition of PM2.5 in lung and extrapulmonary organs. PNAS 116, 2488–2493.

Li, Y., Zhou, J., Rui, X., Zhou, L., Mo, X., 2019b. PM2.5 exposure exacerbates allergic rhinitis in mice by increasing DNA methylation in the IFN-gamma gene promoter in CD4+T cells via the ERK-DNMT pathway. Toxicol Lett 301, 98-107.

Liu, J., Zhang, J., Ren, L., Wei, J., Zhu, Y., Duan, J., Jing, L., Sun, Z., Zhou, X., 2019. Fine particulate matters induce apoptosis via the ATM/P53/CDK2 and mitochondria apoptosis pathway triggered by oxidative stress in rat and GC-2spd cell. Ecotoxicol Environ Saf 180, 280-287.

Mehta, A.J., Zanobetti, A., Bind, M.A., Kloog, I., Koutrakis, P., Sparrow, D., Vokonas, P.S., Schwartz, J.D., 2016. Long-Term Exposure to Ambient Fine Particulate Matter and Renal Function in Older Men: The Veterans Administration Normative Aging Study. Environ Health Perspect 124, 1353-1360.

Meng, X.-M., Tang, P.M.-K., Li, J., Lan, H.Y., 2015. TGF-Î²/Smad signaling in renal fibrosis. Frontiers in Physiology 6.

Meng, X., Huang, X., Chung, A., Qin, W., Shao, X., Igarashi, P., Ju, W., Bottinger, E., Lan, H., 2010. Smad2 protects against TGF-beta_Smad3-mediated renal fibrosis. J Am Soc Nephrol 21, 1477-1487.

Moody, W.E., Edwards, N.C., Madhani, M., Chue, C.D., Steeds, R.P., Ferro, C.J., Townend, J.N., 2012. Endothelial dysfunction and cardiovascular disease in early-stage chronic kidney disease: cause or association? Atherosclerosis 223, 86-94.

Nemmar, A., Al-Salam, S., Al Ansari, Z., Alkharas, Z.A., Al Ahbabi, R.M., Beegam, S., Yuvaraju, P., Yasin, J., Ali, B.H., 2019. Impact of Pulmonary Exposure to Cerium Oxide Nanoparticles on Experimental Acute Kidney Injury. Cell Physiol Biochem 52, 439-454.

Pinkerton, K.E., Green, F.H.Y., Saiki, C., Vallyathan, V., Plopper, C.G., Gopal, V., Hung, D., Bahne, E.B., Lin, S.S., Ménache, M.G., Schenker, M.B., 2000. Distribution of Particulate Matter and Tissue Remodeling in the Human Lung. Environ Health Perspect 108, 1063-1069.

Pope, C.A., 3rd, Bhatnagar, A., McCracken, J.P., Abplanalp, W., Conklin, D.J., O'Toole, T., 2016. Exposure to Fine Particulate Air Pollution Is Associated With Endothelial Injury and Systemic Inflammation. Circ Res 119, 1204-1214.

Rauchman, M., Griggs, D., 2019. Emerging strategies to disrupt the central TGF-beta axis in kidney fibrosis. Transl Res 209, 90-104.

Song, N., Zhang, T., Xu, X., Lu, Z., Yu, X., Fang, Y., Hu, J., Jia, P., Teng, J., Ding, X., 2018. miR-21 Protects Against Ischemia/Reperfusion-Induced Acute Kidney Injury by Preventing Epithelial Cell Apoptosis and Inhibiting Dendritic Cell Maturation. Front Physiol 9, 790.

Stam, F., van Guldener, C., Becker, A., Dekker, J.M., Heine, R.J., Bouter, L.M., Stehouwer, C.D., 2006. Endothelial dysfunction contributes to renal function-associated cardiovascular mortality in a population with mild renal insufficiency: the Hoorn study. J Am Soc Nephrol 17, 537-545.

Su, R., Jin, X., Zhang, W., Li, Z., Liu, X., Ren, J., 2017. Particulate matter exposure induces the autophagy of macrophages via oxidative stress-mediated PI3K/AKT/mTOR pathway. Chemosphere 167, 444-453.

Tanase, D.M., Gosav, E.M., Radu, S., Costea, C.F., Ciocoiu, M., Carauleanu, A., Lacatusu, C.M., Maranduca, M.A., Floria, M., Rezus, C., 2019. The Predictive Role of the Biomarker Kidney Molecule-1 (KIM-1) in Acute Kidney Injury (AKI) Cisplatin-Induced Nephrotoxicity. Int J Mol Sci 20.

Tavera Busso, I., Mateos, A.C., Juncos, L.I., Canals, N., Carreras, H.A., 2018. Kidney damage induced by sub-chronic fine particulate matter exposure. Environ Int 121, 635-642.

Verma, S.K., Molitoris, B.A., 2015. Renal endothelial injury and microvascular dysfunction in acute kidney injury. Semin Nephrol 35, 96-107.

Wang, J.S., Tseng, C.Y., Chao, M.W., 2017a. Diesel Exhaust Particles Contribute to Endothelia Apoptosis via Autophagy Pathway. Toxicol Sci 156, 72-83.

Wang, W., Deng, Z., Feng, Y., Liao, F., Zhou, F., Feng, S., Wang, X., 2017b. PM2.5 induced apoptosis in endothelial cell through the activation of the p53-bax-caspase pathway. Chemosphere 117, 135-143.

Wang, W., Zhou, J., Chen, M., Huang, X., Xie, X., Li, W., Cao, Q., Kan, H., Xu, Y., Ying, Z., 2018. Exposure to concentrated ambient PM2.5 alters the composition of gut microbiota in a murine model. Part Fibre Toxicol 15, 17.

Xu, Y., Wang, W., Zhou, J., Chen, M., Huang, X., Zhu, Y., Xie, X., Li, W., Zhang, Y., Kan, H., Ying, Z., 2019. Metabolomics analysis of a mouse model for chronic exposure to ambient PM2.5. Environ Pollut 247, 953-963.

Yan, Y.H., C, C.K.C., Wang, J.S., Tung, C.L., Li, Y.R., Lo, K., Cheng, T.J., 2014. Subchronic effects of inhaled ambient particulate matter on glucose homeostasis and target organ damage in a type 1 diabetic rat model. Toxicol Appl Pharmacol 281, 211-220.

Zhang, J., Liu, J., Ren, L., Wei, J., Duan, J., Zhang, L., Zhou, X., Sun, Z., 2018a. PM2.5 induces male reproductive toxicity via mitochondrial dysfunction, DNA damage and RIPK1 mediated apoptotic

signaling pathway. Sci Total Environ 634, 1435-1444.

Zhang, Y., Hu, H., Shi, Y., Yang, X., Cao, L., Wu, J., Asweto, C.O., Feng, L., Duan, J., Sun, Z., 2017. (1)H NMR-based metabolomics study on repeat dose toxicity of fine particulate matter in rats after intratracheal instillation. Sci Total Environ 589, 212-221.

Zhang, Y., Li, S., Li, J., Han, L., He, Q., Wang, R., Wang, X., Liu, K., 2018b. Developmental toxicity induced by PM2.5 through endoplasmic reticulum stress and autophagy pathway in zebrafish embryos. Chemosphere 197, 611-621.

Zhang, Y.H., Zhang, Y.Q., Guo, C.C., Wang, L.K., Cui, Y.J., Dong, J.J., Liao, L., 2019. Prostaglandin E1 attenuates high glucose-induced apoptosis in proximal renal tubular cells by inhibiting the JNK/Bim pathway. Acta Pharmacol Sin.

Zhou, B., Liang, G., Qin, H., Peng, X., Huang, J., Li, Q., Qing, L., Zhang, L., Chen, L., Ye, L., Niu, P., Zou, Y., 2014. p53-Dependent apoptosis induced in human bronchial epithelial (16-HBE) cells by PM(2.5) sampled from air in Guangzhou, China. Toxicol Mech Methods 24, 552-559.

Zhou, T., Hu, Y., Wang, Y., Sun, C., Zhong, Y., Liao, J., Wang, G., 2019. Fine particulate matter (PM2.5) aggravates apoptosis of cigarette-inflamed bronchial epithelium in vivo and vitro. Environ Pollut 248, 1-9.

Zhou, Z., Shao, T., Qin, M., Miao, X., Chang, Y., Sheng, W., Wu, F., Yu, Y., 2018. The effects of autophagy on vascular endothelial cells induced by airborne PM2.5. J Environ Sci (China) 66, 182-187.

Figures

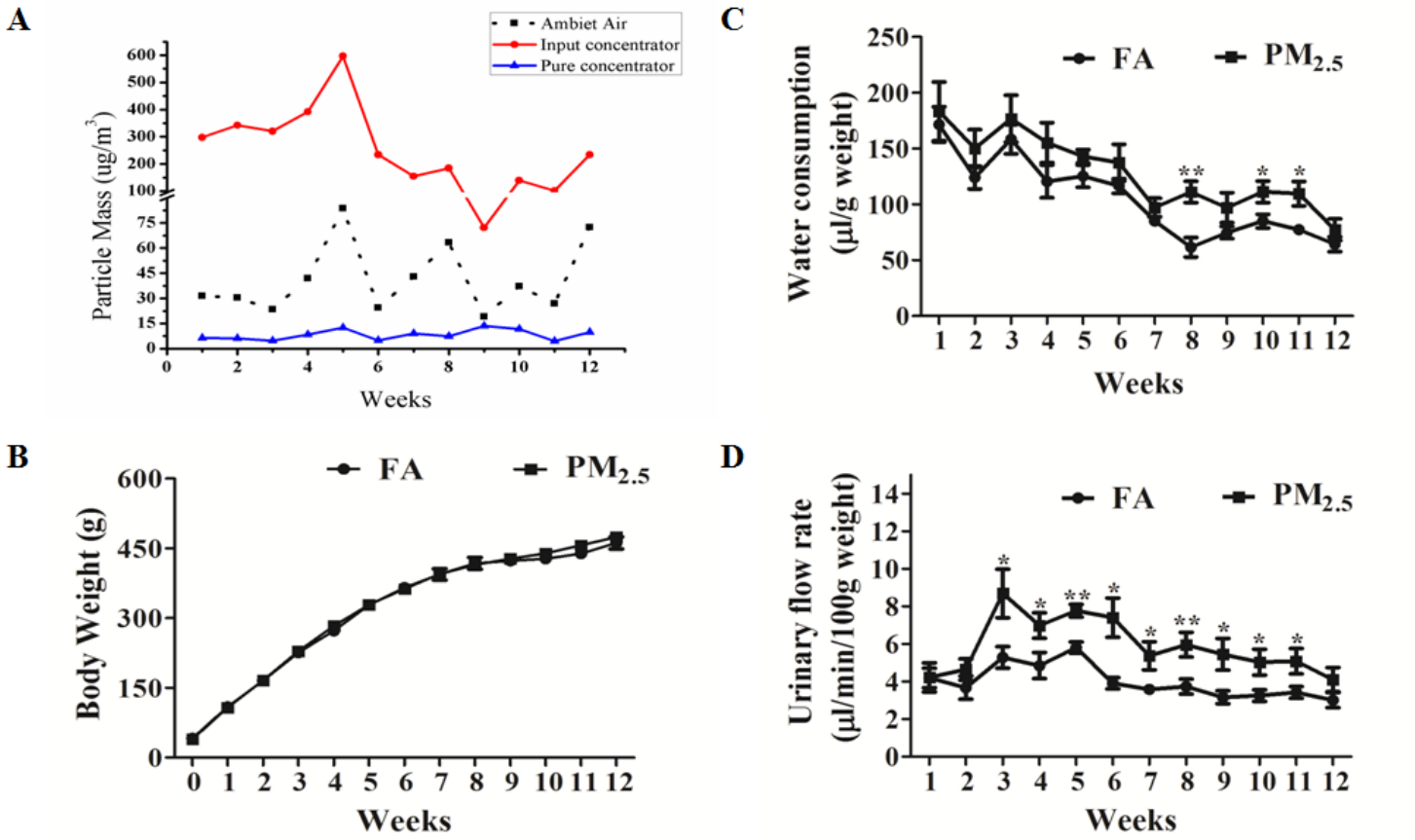

Figure 1

PM2.5 concentration monitoring and the effects of PM2.5 on the physiological metabolism in rats. A. During the exposure period, the mean PM2.5 concentrations of ambient air, exposure chamber and control chamber were monitored simultaneously, 5- day per week and 8-hour per day. B. Changes in rats' body weight during exposure period. C. The water consumption during 24-hour period in the metabolic cages. D. Urinary flow rates during 24-hour in the metabolic cages. Values are significantly compared to FA group: *p < 0.05, **p<0.01.

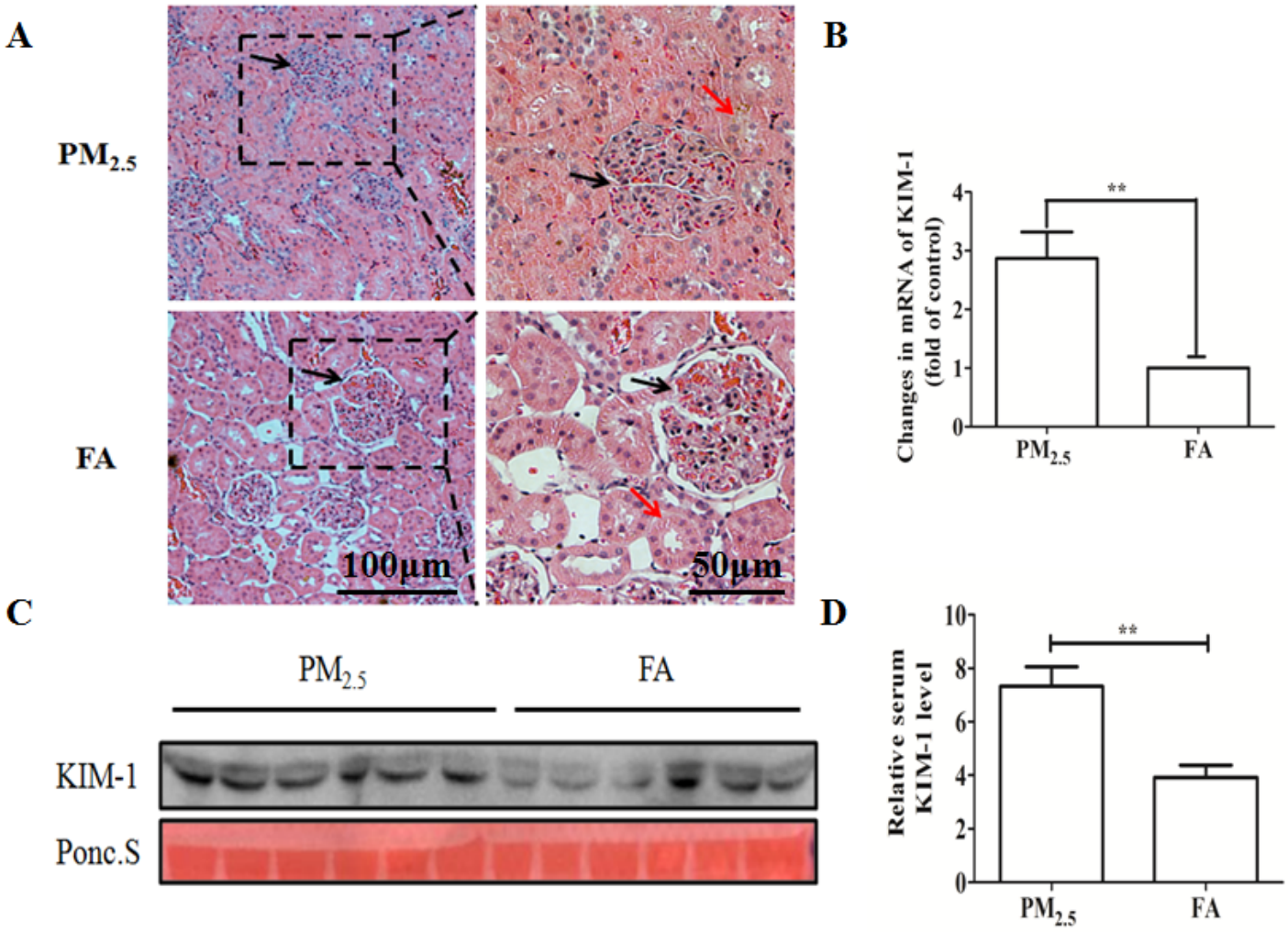

Figure 2

Renal histopathologic changes caused by PM2.5 exposure. A. H&E staining of renal tissue (glomerulus marked by black arrow and renal tubules marked by the red arrow). B. RT-PCR analysis of KIM-1 in kidney cortex. C-D. WB analysis of KIM-1 in serum, on histogram graphic** indicates statistical difference ($p<0.01$).

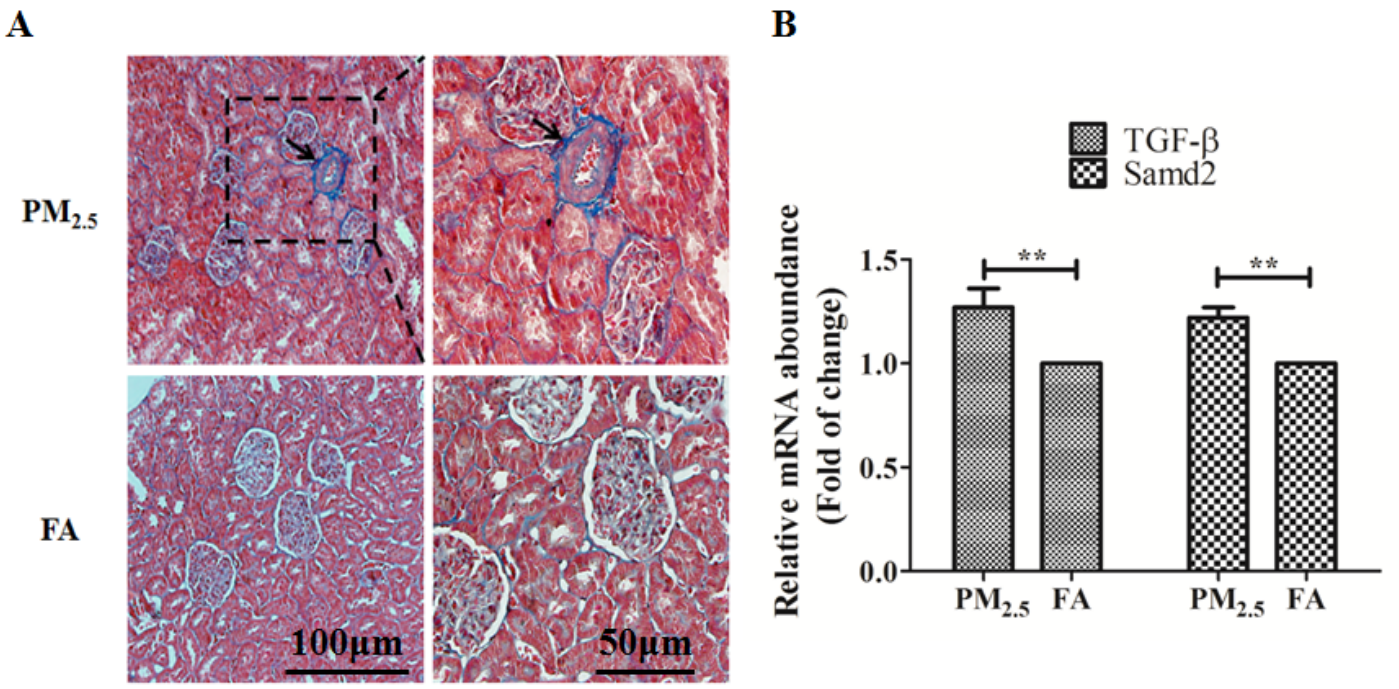

Figure 3

Collagen deposition induced by PM2.5 exposure. A. Deposit of collagen by Masson's Trichromic staining. B. mRNA expressions of TGF-β and Smad2, on histogram graphic** indicate statistical difference ($p<0.01$).

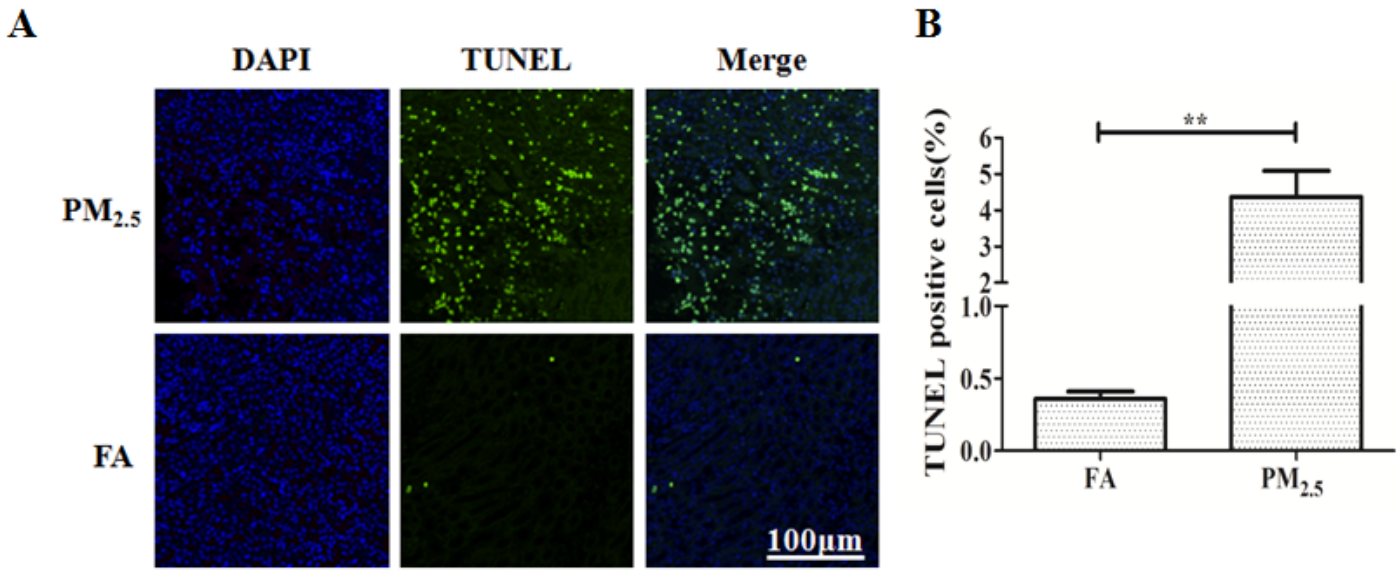

Figure 4

TUNEL analysis of rats kidney tissues. A. Representative images are showing cell apoptosis in renal tissues induced by PM2.5. B. Statistical analysis of the proportion of apoptosis cells. Cells with green light presented TUNEL positive cells, on histogram graphic** indicates statistical difference ($p<0.01$).

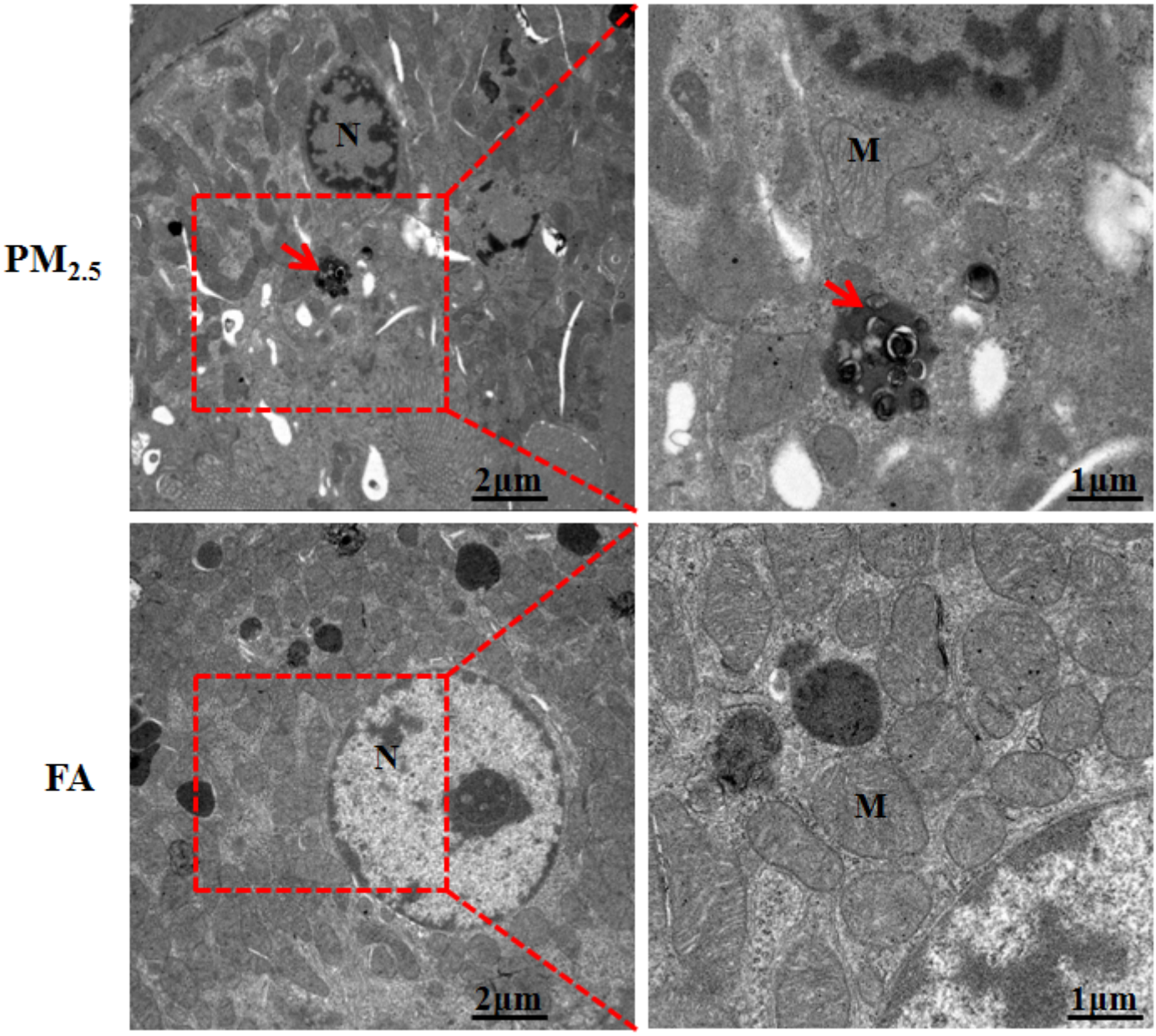

Figure 5

TEM images of kidney tissues after PM2.5 exposure. Representative images showing changes in the microscopic structure of renal tissue cells. N means the nucleus, M means the mitochondria, and arrows indicates multilayered (myeloid) matter.

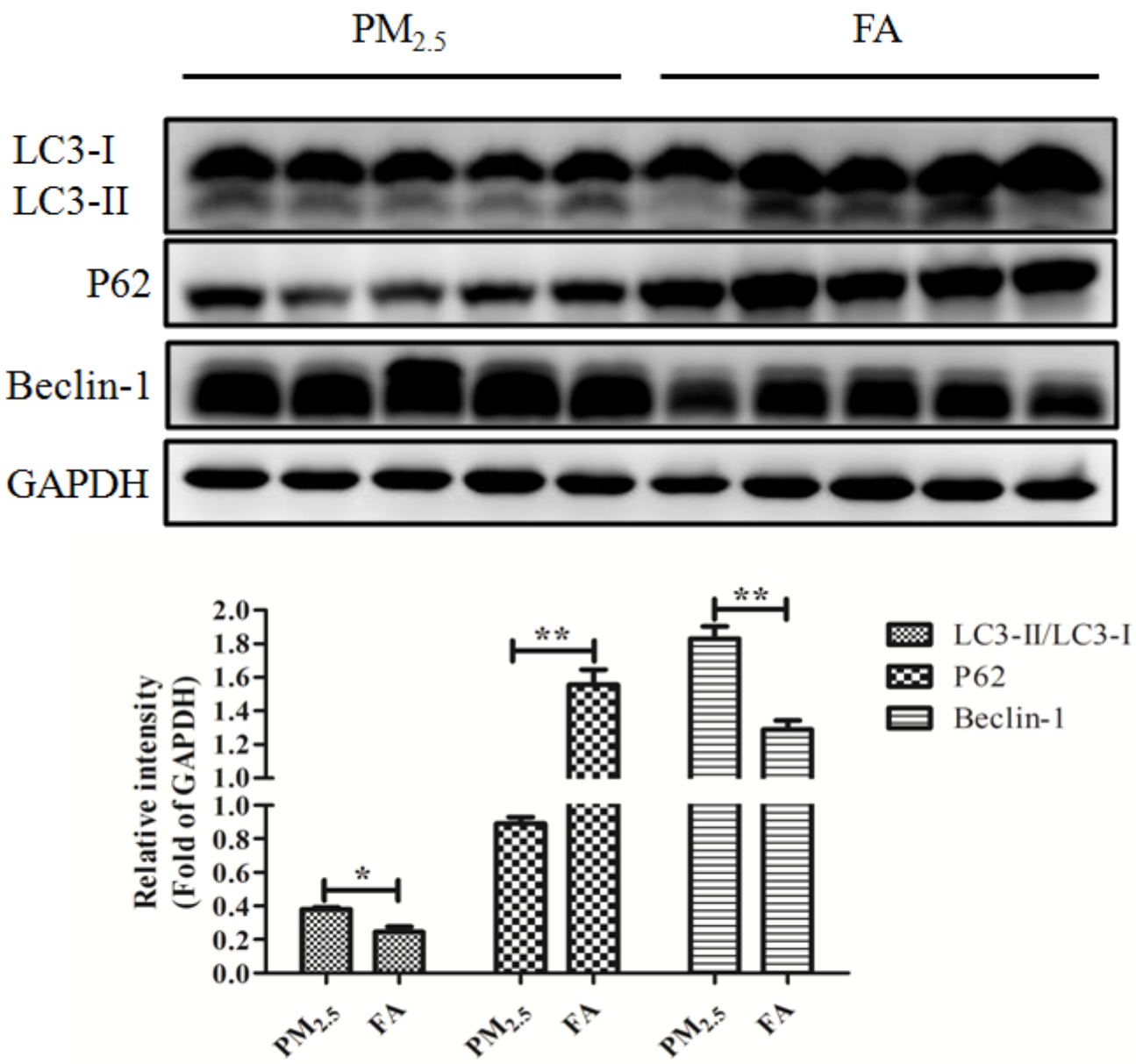

Figure 6

Activation of autophagic pathway after PM2.5 exposure in rats. Western blots and quantitative expressions of LC3, Beclin-1and P62. GAPDH was used as the loading control.

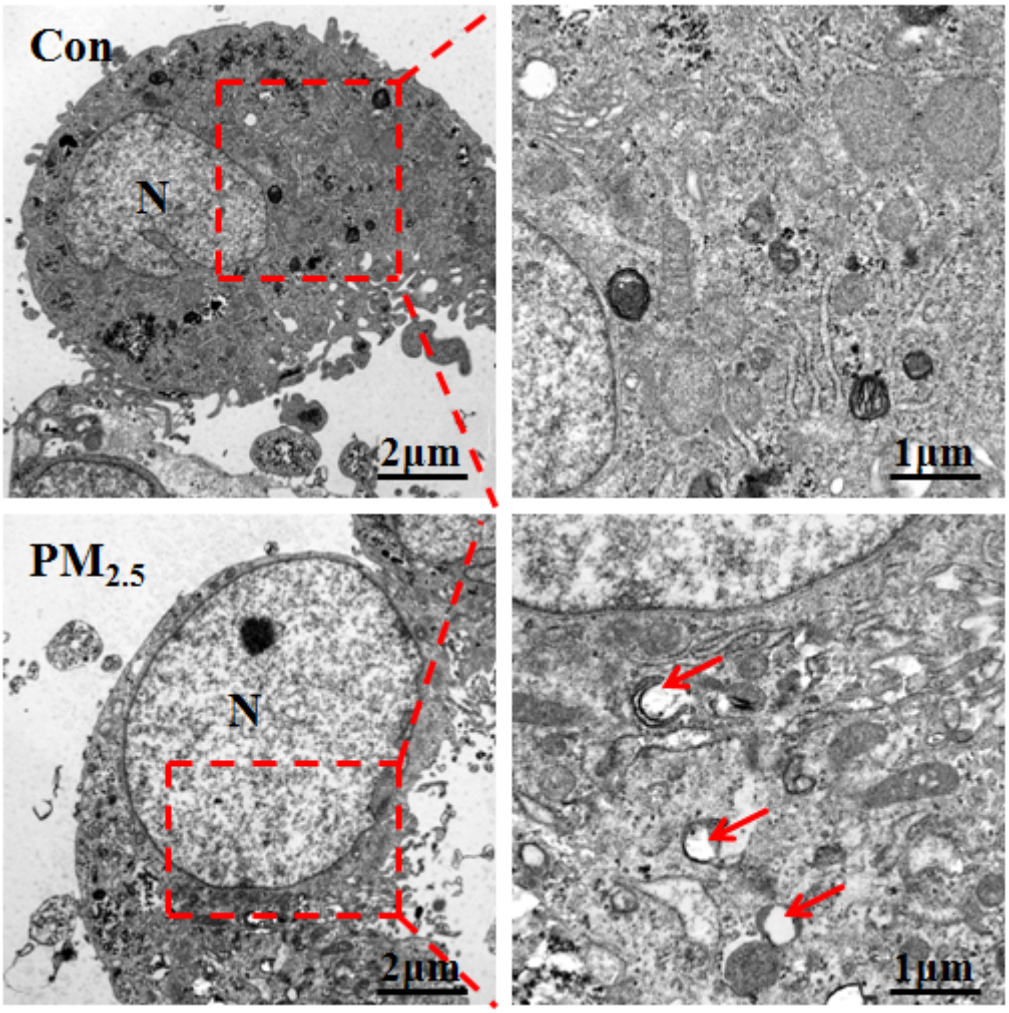

Figure 7

Effects of PM2.5 exposure on cell morphology and autophagy in HK-2 cells. TEM images showing morphological changes and autophagosomes in PM2.5 (400 μg/mL) treated HK-2 cells. Red arrows indicate autophagosomes. N, nucleus.

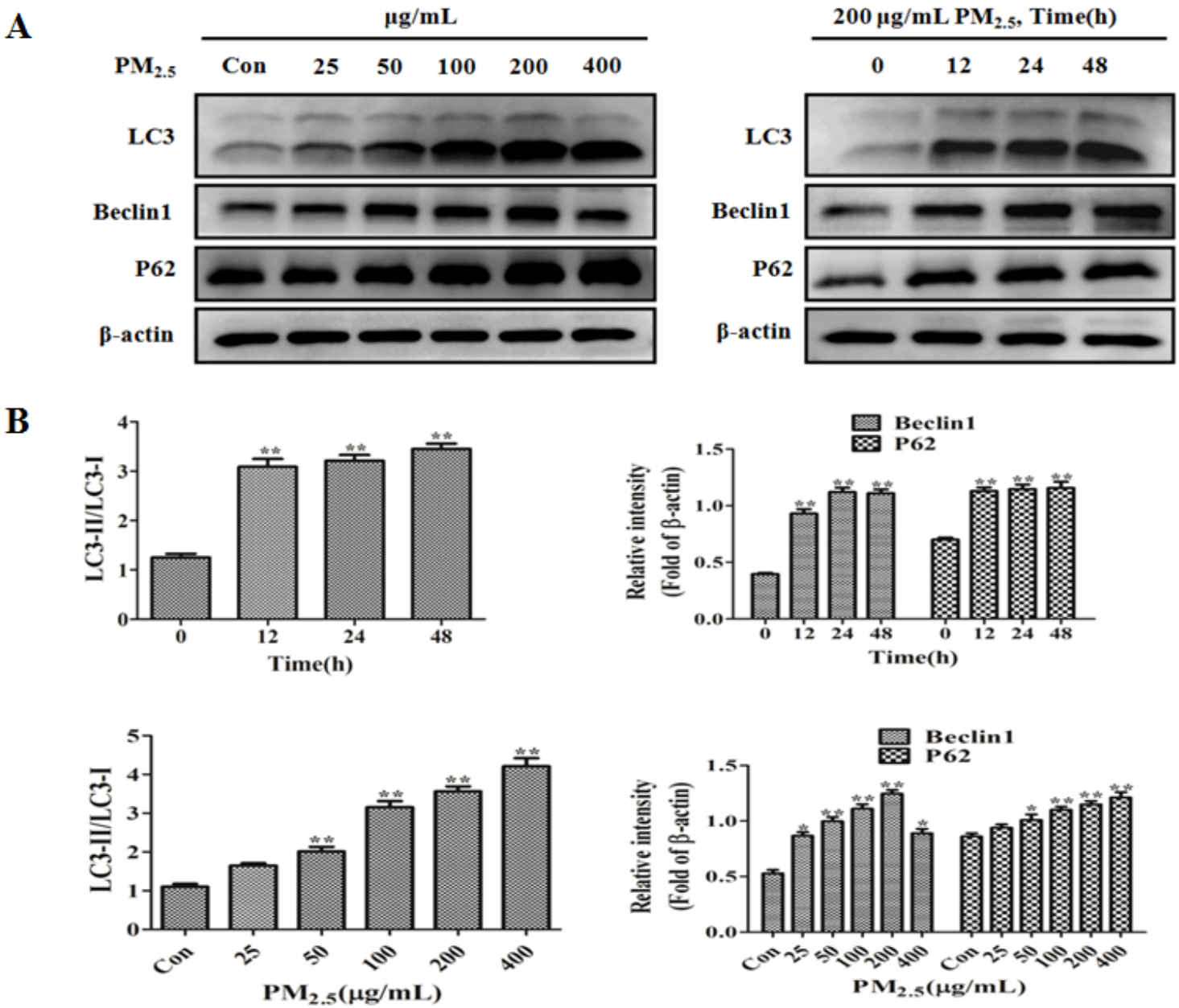

Figure 8

Activation of autophagic pathway caused by PM2.5 in HK-2 cells. A-D Western blots and quantitative expressions of LC3, Beclin-1and P62. β-actin was used as the loading control.